SPATIAL VARIABILITY AND SOURCE-RECEPTOR RELATIONS AT A STREET INTERSECTION

ALAN ROBINS[1*], ERIC SAVORY[1], ATHENA SCAPERDAS[2] and DIMOKRATIS GRIGORIADIS[3]

[1] *School of Engineering, University of Surrey, Guildford, Surrey, U.K.;* [2] *WS Atkins Engineering Science Ltd, Woodecote Grove, Epsom, Surrey, U.K.;* [3] *NCSR Demokritos, 153 10 Aghia Paraskevi, Attiki, Greece*

(author for correspondence, e-mail: a.robins@surrey.ac.uk, fax: +44 (0) 1483 259546)*

Abstract. A wind tunnel study of dispersion at a simple urban intersection comprising two perpendicular streets is described. Concentration and flow field measurement were undertaken to determine the importance of the exchange of pollutants between the streets and to investigate source-receptor relationships at the intersection. The results showed that only in a symmetrical situation were exchanges negligible and that small departures from symmetry, brought about in the experiments through an off-set in the street alignment or a change of orientation relative to the wind, were sufficient to establish significant exchanges. The results also showed that significant structure appeared in the concentration fields in the streets as a result. Examples are shown where concentrations on one side of a street are entirely due to emissions from the perpendicular street, whereas on the opposite side concentrations depend on emission upwind in the same street as the receptor. The results imply that exchanges between street systems are likely to be the norm in practice and that the consequences of such exchanges are not confined to the immediate vicinity of the intersection.

Keywords: air quality, dispersion modelling, intersections, street-canyons

1. Introduction

The study of line sources in 'urban street canyons' has dominated short range dispersion research in urban areas. However, a number of studies (e.g. Hoydysh and Dabberdt, 1994; Scaperdas, 2000; Soulhac, 2000) have shown the importance of three dimensional effects at intersections, in particular the exchange of air, and hence pollutants, between the street systems involved. Air exchanges can be quantified through flow field measurements (or predictions) whereas pollutant transfers are most easily understood by using point sources at various locations within the street systems near the intersection.

Figure 1 is based on one of the cases investigated by wind tunnel simulation by Scaperdas (2000). It shows the measured flow interchanges at a simple intersection between two perpendicular streets. The approaching flow is along the 'x-street' and there is a lateral off-set at the intersection of $\Delta y = 0.6$ H, where H is the height (125 mm) of the four blocks used to define the intersection; the street width is also

Water, Air, and Soil Pollution: Focus **2:** 381–393, 2002.

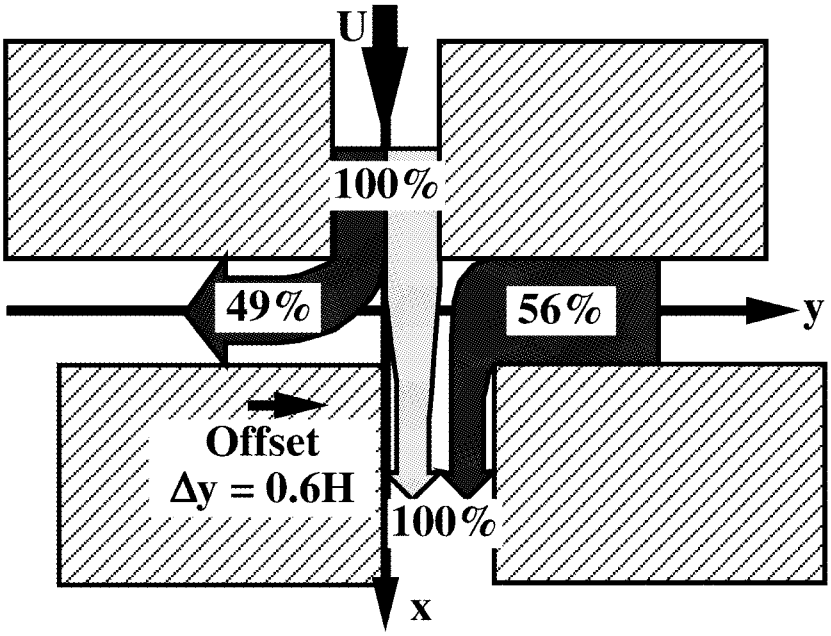

Figure 1. Flow interchanges at an intersection defined by four blocks of height H, with a 0.6 H off-set. Block size 6 H×4 H.

H in this case. The arrows and labels mark the volume flux exchanges relative to the volume flux in the upwind x-street (denoted as 100%). Clearly, a considerable flow of air passes into the y-street (in the section $y < 0$) from the upwind part of the x-street ($x < 0$). Such exchanges and the mechanisms associated with them lead to:

1. significantly larger pollutant source terms in the y-street than would otherwise be expected;
2. marked spatial structure in concentration distributions near the intersection; and
3. the development of high levels of concentration fluctuations.

particularly when the traffic flows in the×and y-streets are different. The objectives of the work discussed in this article were to explore these matters in further detail and to provide comprehensive sets of data for testing the predictive ability of numerical methods. Here, we concentrate on the former.

2. Methodology

The experiments were undertaken in the EnFlo Meteorological Wind Tunnel at the University of Surrey, which has a 20×3.5×1.5 m high working section and can be

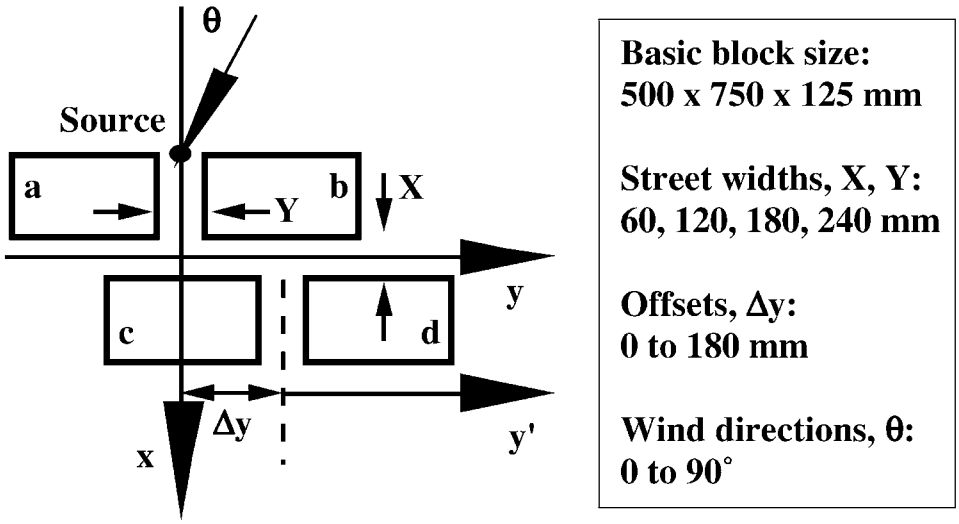

Figure 2. Schematic diagram of model arrangements including definitions of axes, orientation and off-set.

used to simulate a wide range of stable, neutral and unstable boundary layers. In this work only neutral flow was considered. The approach flow was a 1 m deep neutral boundary layer with friction velocity u_*/U_{ref} = 0.055, where U_{ref} is the wind speed at the boundary layer edge, and surface roughness length, z_o = 1 mm. The building blocks were 125 mm high and 750×500 mm in plan, arranged as shown in Figure 2, with off-sets from 0 to 1.5 H. Wind directions, as defined in the figure, from 0° to 90° were investigated. The experiments were carried out at reference speeds in the range from 2 to 2.5 ms^{-1}, and the characteristic Reynolds number, HU_{ref}/ν, was of order 20 000.

The four blocks stood alone in the tunnel – they were not part of a 'larger' urban array. This configuration was chosen as a test case for CFD work because it provides particularly simple boundary conditions and is not excessively demanding on grid design. The block size ensures that the flow over the roof reattaches well upstream of the separation at the trailing edge, so that the flow above the street canyon is essentially horizontal. The ratio H/z_o was about 125, whereas figures in the range from 10 to 30 are more typical of urban areas. This is not a significant mis-match as concern rests in generic features of the flow within the street canyon, not in the structure of the boundary layer above the buildings. For similar reasons, no great significance attaches to the relatively shallow boundary layer used in the wind tunnel.

The distribution of mean concentration within the street network was measured with flame ionisation detector based instrumentation, trace gas being released from a (nominally) point source at ground level. Line source results were calculated from the point source data. A multi-channel sampling and analysis system was used for

TABLE I

Measured flow exchanges at the intersection, expressed as a percentage of the flow from the upwind street, Q_1

Off-set	Orientation	Relative volume flux towards intersection (%)			
Δy/H	θ°	Q_1 (x < 0)	Q_2 (x > 0)	Q_3 (y < 0)	Q_4 (y > 0)
0	0	100	–112	6	6
0.1	0	100	–110	–9	20
0.6	0	100	–100	–49	56
0	10	100	–95	–9	32

mean concentration measurement and two Cambustion Fast FIDs for fluctuation measurement. Sources were positioned on the centre line of the×and y-streets. A two component laser-Doppler anemometer was used to map the velocity field in a limited number of cases. Quantitative measurements were preceded by comprehensive flow visualisation studies that were used to gain insight into the dispersion processes and to guide the selection of cases for subsequent detailed study.

3. Results

All the results discussed in this section were measured at a height of H/6 above street level; i.e. they describe street-level conditions.

3.1. Exchanges at the intersection

The exchanges between the streets at the intersection were calculated from measurements of the distribution of mean velocity over planes near the intersection that were perpendicular to the streets. Table I lists the relative volume flux exchanges for four arrangements, specified in terms of the off-set, Δy, and orientation, θ. Fluxes are positive into the intersection and expressed as percentages of Q_1, the flux from the upwind street,×< 0; Q_2 is the flux from the downwind street,×> 0, Q_3 from y < 0 and Q_4 from y > 0. Any imbalance is due to experimental error and vertical exchange.

In the first case, $\Delta y = \theta = 0$, there is no asymmetry to create secondary flow and the weak flux from the y-street into the x-street is driven by mixing at the intersection. As will be seen later, this mean flow masks the fact that mixing transfers some pollutant from the x-street into the y-streets. An off-set as small as 0.1H is sufficient to create well defined secondary flows in the lateral streets, with significant transfer from the upwind x-street into the left lateral street (y < 0), and from the right lateral (y > 0) into the downwind x-street. Increasing the offset to 0.6 H

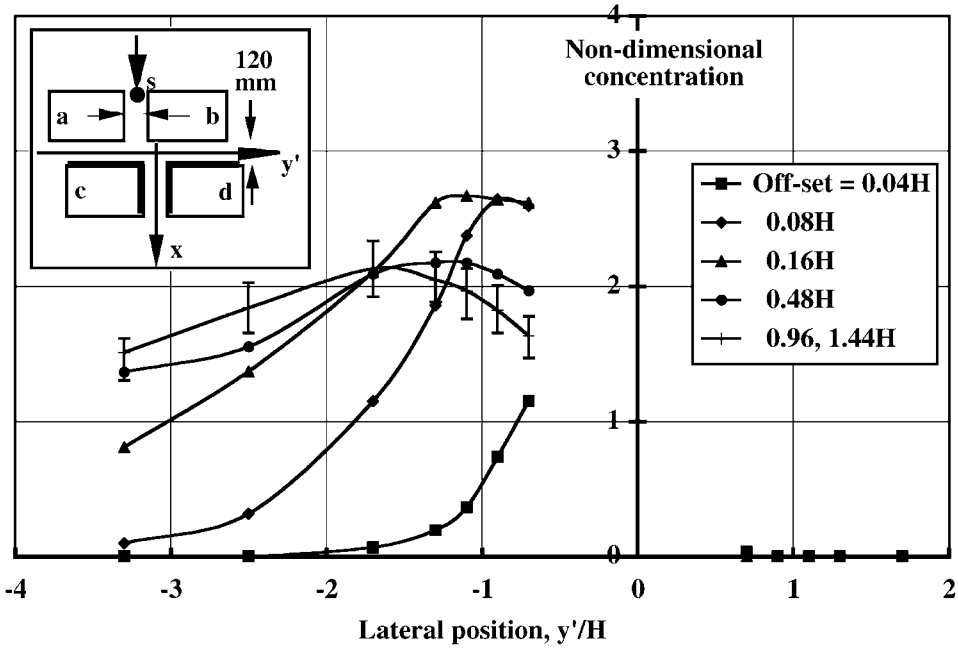

Figure 3. Non-dimensional concentration profiles along lateral streets at x = –0.5 H for $\theta = 0°$ and off-sets $\Delta y = 0.04$ H to 1.44 H; the source was located at the entrance to the upwind street and y' is measured from the centre of the downwind street.

produces the results shown in Figure 1, with approximately 50% of the flow from the upwind street passing into the left lateral street and a somewhat larger flow from the right lateral into the downwind street. In circumstances like this the pollutant flux from the upwind street would be relatively large, because the mean flow is along the street, and would provide a substantial source term in the lateral street. The lateral street would generally be modelled as a street-canyon with wind normal to it, and clearly the flux from the intersection will completely change the character of the concentration field within the street. How far such changes penetrate into the lateral street is discussed later. Larger exchanges between the street systems are also observed in the case $\Delta y = 0$, $\theta = 10°$, though in this case there is a substantial imbalance in the horizontal fluxes. Whether this is due to experimental error or indicates a large vertical flux into the flow above the buildings is not known. Both this and the $\Delta y/H = 0.1$, $\theta = 0°$ case show that behaviour is very sensitive to small perturbations (as always exist in reality), a point returned to later.

3.2. Concentration distributions

Figure 3 shows measurements of mean concentration, C (0.5 H, y', 0.16 H), along the downwind side (x = 0.5 H) of the lateral streets for a point source in the upwind street at x/H = –4; results for an off-set of 1.44 H were virtually identical to those

TABLE II

The four receptors chosen for the discussion of source-receptor relationships

Receptor location			Description
x/H	y/H	z/H	
1.38	–0.32	0.16	A pair on either side of the x-street, 0.9 H from the street entrance.
1.38	0.64	0.16	
0.48	–1.12	0.16	A pair on the downwind side of the y-street, 0.64 H from the entrance
0.48	1.04	0.16	to each segment.

shown for 0.96 H. Concentrations are plotted in non-dimensional form, $CU\mathrm{H}^2/Q$ (where U is the wind speed in the undisturbed flow at height H and Q is the source strength), as a function of position, y′/H, measured relative to the centre of the downwind street. Error bars are included for the 0.96 H off-set data and these are typical of all results. The rapid increase of penetration into the left lateral street ($y' < 0$) with increasing off-set is clear, whilst concentrations in the right lateral street ($y' > 0$) are zero. Maximum concentration levels are of the same magnitude as those near the intersection in the x-street. These results are entirely consistent with the flow patterns illustrated in Figure 1. Significant concentrations occurred throughout the lateral street (in these experiments of length 6 H), suggesting that nowhere within it were conditions attained for valid application of a standard street-canyon model with wind normal to the street.

Results for zero off-set have not been included in Figure 3. Measurement repeatability in this symmetrical arrangement proved to be much worse than usual and very sensitive to minor perturbations to the model set-up in the wind tunnel. Breaking the symmetry, even by as little as an off-set of 0.04 H, was sufficient to eliminate the high run-to-run variability and restore the expected level of repeatability. However, significant concentration levels were not measured beyond $|y'/H| = 1$, though this was the only case investigated where concentrations were observed in both segments of the lateral street.

3.3. Source-receptor relationships

Mean concentrations were measured at a fixed set of receptor locations, each approximately 1 to 1.5 H from the centre of the intersection, for a range of ground level point source positions along the × and y axes for the model arrangement $\Delta y/H = 0.16$, $\theta = 0°$. Four receptor locations, chosen to illustrate the characteristic features of dispersion behaviour at the intersection, will be used to the discuss source-receptor relationships. The selected receptors are described in Table II and the results are present in Figures 4 and 5.

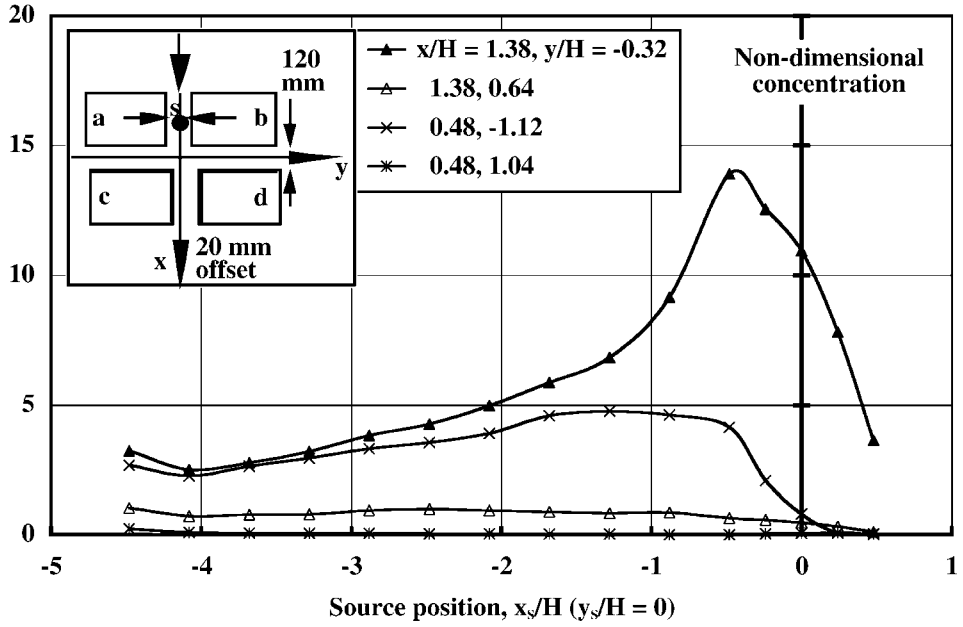

Figure 4. Receptor concentrations at four selected locations as a function of the source position in the x-street, $\Delta y/H = 0.16$, $\theta = 0°$.

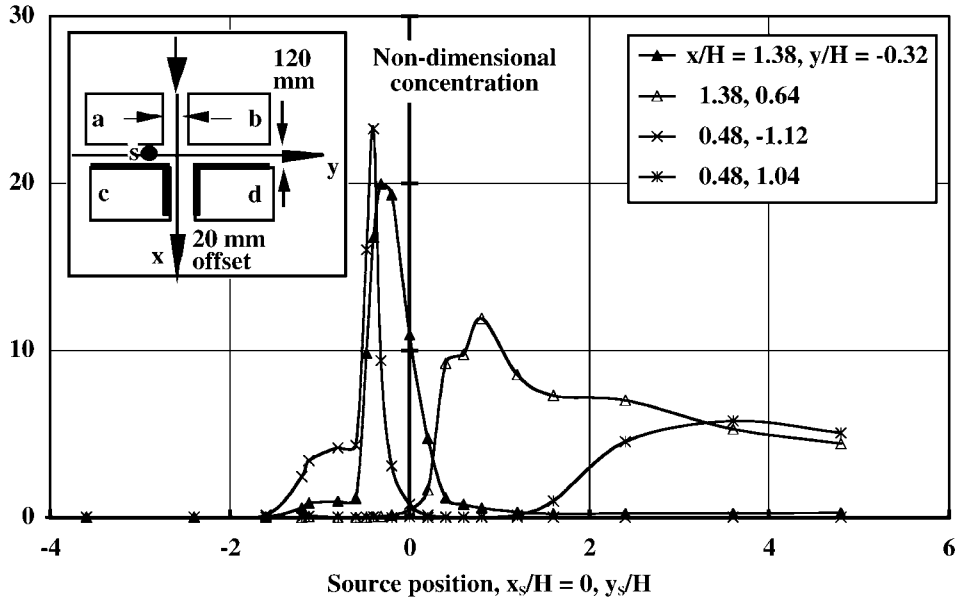

Figure 5. Receptor concentrations at four selected locations as a function of the source position in the y-street, $\Delta y/H = 0.16$, $\theta = 0°$.

Figure 4 treats sources in the x-street. Concentrations measured on either side of the downwind sector of the x-street (x/H = 1.38, y/H = –0.32 and 0.64) reveal considerable differences. The highest concentration shown occurs at the first of these locations when the source is at x_s/H≈–0.5. Thus in travelling approximately 2 H the plume has dispersed sufficiently to generate the maximum street-side concentration; plume spread and lateral displacement are both likely to be important in this process. The second of this pair of locations is affected by the clean air that comes from the right hand lateral street, as illustrated in Figure 1. The resulting cross-street structure persists far into the x-street and is little reduced at x = 4 H, the final receptor position studied. Concentrations in the left side of the lateral street are advected from the upwind x-street and decay quite slowly with fetch along the street. Concentrations fall as the source moves downstream from about the centre of the intersection because material then no longer reaches the receptor point by advection and diffusion across the street. Concentrations are zero in the other half of the lateral street since it is exposed solely to clean air flowing along it in the negative y direction.

Figure 5 treats the same receptors, but for sources located in the y-street. The pattern is now quite different, with sharp peaks arising at two of the locations when the source is near the intersection. These occur at the receptors at x/H = 1.38, y/H = –0.32 and 0.48, –1.12 when the source position is in the range from y_s/H≈0 to –0.8, indicating direct advection of the plume from source to receptor. The first of these receptors is only affected for a narrow range of source positions as might be excepted from the flow fields sketched in Figure 1. There is some evidence of dispersion counter to the overall mean flow direction in that concentrations are observed at this receptor even when the source is at y_s/H = –1. In contrast, the opposite receptor (x/H = 1.38, y/H = 0.64) is exposed to pollutant from all source positions in the right hand segment of the lateral street and no source positions in the left hand segment, again reflecting the flows sketched in Figure 1.

The sharpest peak in the concentration distributions occurs for the receptor in the right hand lateral street (x/H = 0.48, y/H = –1.12). No material from the other segment of the street reaches this position and there is no evidence of dispersion counter to the overall mean flow since concentrations fall to zero when $y_s < y$. This, together with the observations discussed above, suggests that y_s/H≈–1.2 is approximately the limiting source position from which material can disperse into the downwind x-street. Concentrations are only observed at the receptor in the other section of the lateral street, where y > 0, when the source is upstream of the receptor in terms of the secondary flow within the street.

3.4. LINE SOURCES

Line source results can be synthesised from the point source data to quantify the relative contributions from each street to concentrations at a given receptor. We assume that the concentration, C_{Ln}, at a given receptor due to emissions from the

TABLE III
Receptor positions for analysis of line source results

Receptor	x/H	y/H	Receptor	x/H	y/H
Lateral street at z/H = 1/6					
1	0.48	–2.12	4	0.48	–0.53
2	0.48	–1.12	5	0.48	0.84
3	0.48	–0.72	6	0.48	1.04
Longitudinal street at z/H = 1/6					
7	3.68	–0.32	12	0.68	0.64
8	2.48	–0.32	13	0.88	0.64
9	1.28	–0.32	14	1.28	0.64
10	0.88	–0.32	15	2.48	0.64
11	0.68	–0.32	16	3.68	0.64

'nth' element of the line source, length λ_n, can be written as follows in terms of the concentration, C_n, from a point source at the centre of the element:

$$C_{Ln}U\mathrm{H}/q = (CU\mathrm{H}^2/Q)_n(\lambda_n/\mathrm{H}) ,$$

where q is the line source strength per unit length and Q the point source strength. Summing over all such elements gives the concentration due to the line source, C_L:

$$C_L U\mathrm{H}/q = \Sigma_n(CU\mathrm{H}^2/Q)_n(\lambda_n/\mathrm{H}) .$$

In this way results can be derived for a line source along the longitudinal street from x/H = –4.48 to 0.48 and a second line source along the lateral street from y/H = –4.8 to 4.8. The section of each line source that provides the main contribution to the concentration levels at a given receptor can also be determined.

Figure 6 shows non-dimensional concentrations, $C_L U\mathrm{H}/q$, at the 16 receptor positions specified in Table III, assuming equal source strengths for the two line sources. The contribution from each line source is shown separately. Receptors 1 to 4 are in the left lateral street (y < 0) and here both line sources contribute, with the x line source responsible for about 2/3 of the total near the intersection. By contrast, the two receptors, 5 and 6, in the other segment of the lateral street (y > 0) are only influenced by sources in the same segment because the mean flow is along the street towards the intersection. There is also a strong contrast between the two sides of the longitudinal street (x > 0). The left hand side (y < 0) receptors (7 to 11) are largely affected by the line source in the same street, with only about 1/4 of the total derived from the y line source, whereas concentrations on the right

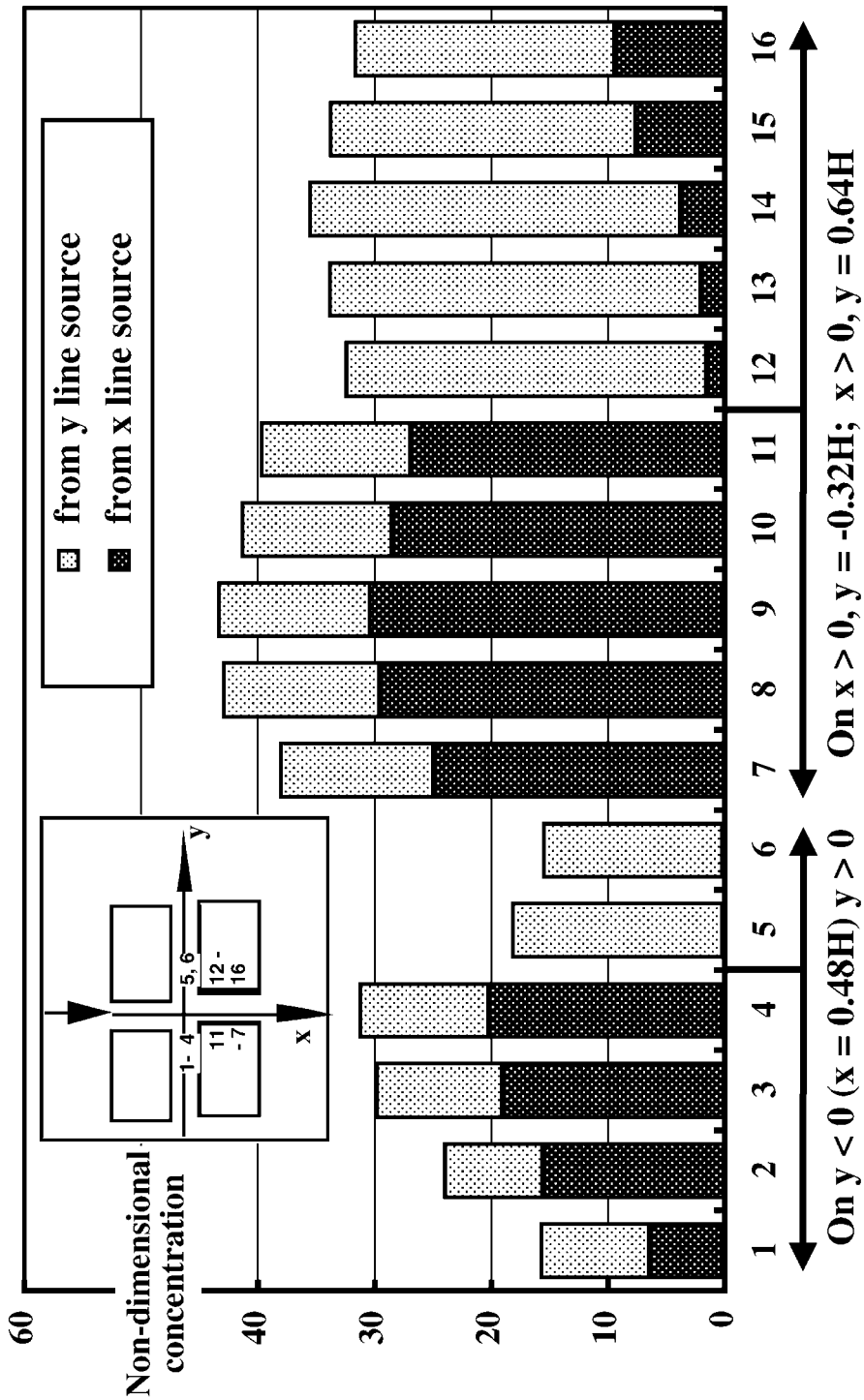

Figure 6. Contributions to pollutant levels at the 16 receptors for equal strength×and y line source emissions; $\Delta y/H = 0.16$, $\theta = 0°$.

TABLE IV

The 'active' lengths of the line sources affecting each receptor

Receptor location			Longitudinal line source		Lateral line source	
x/H	y/H	z/H	x_{s10}/H	x_{s90}/H	y_{s10}/H	y_{s90}/H
1.28	–0.32	0.17	–3.2	–0.1	–0.5	0.4
1.28	0.64	0.17	–3.8	–0.6	0.7	3.5
0.48	–1.12	0.17	–3.6	–0.8	–1.0	–0.3
0.48	1.04	0.17	–[a]	–[a]	2.5	4.5

[a] No measurable concentrations due to longitudinal line source.

(receptors 12 to 16) are dominated by the y line source. The situation scarcely changes with increasing distance along the street, the only significant development being a gradual increase in the contribution from the x line source on the right hand side of the street.

A convenient measure of the 'active' length of a line source is the extent responsible for, say, 80% of its contribution to the mean concentration at a receptor. This can be specified by end points x_{s10} and x_{s90} for the x line source (defined such that 10% contributions derive from $x_s < x_{s10}$ and $x_s > x_{s90}$) and y_{s10} and y_{s90} for the y line source. Table IV presents such active length data for the four receptors previously discussed (numbers 2, 6, 9 and 14 in Table III). The results contrast two cases with a relatively short active length (of order H), with two where the active length is of order 3 H long. The former correspond to the narrow peaks seen in Figure 5, which are associated with the direct advection of the plume from its source to a receptor. These are the only situations shown where concentrations would not increase were the line sources made more extensive (apart from the trivial case in Figure 4 where concentrations are zero for all source locations).

4. Discussion

The results clearly reveal the importance of the transfer of pollutants from one street to the other at an intersection and show that this becomes significant as soon as there are minor departures from symmetry in the geometry. The magnitude of the fluxes involved is very sensitive to the local geometry, in these experiments the magnitude of the off-set, and the wind direction. One implication is that such transfers are likely to be the norm at urban street intersections. The experiments also show that the consequences of such transfers are not confined to the immediate vicinity of the intersection and may penetrate far into the streets involved. The sensitivity to small changes in geometry is also associated with a high level of long time scale concentration fluctuations near the intersection, as was first observed during initial flow visualisation studies and later revealed in detail by fluctuation

measurements (to be published at a later date). In practice, such fluctuations may be greatly enhanced by the unsteadiness in the source terms that results from the characteristics of the traffic and its movement. However, this does not affect the mean concentrations discussed in this article since all that is required for their evaluation is appropriate mean source terms.

Integral models can be readily written for flow and dispersion along the streets comprising the intersection. These can be designed so that they tend to a standard street-canyon model (e.g. Berkowicz *et al.*, 1997) far from the intersection, though something simpler serves as an illustration. Define C and U_S as the average concentration and mean flow speed within a street canyon in a plane normal to the street, where U_S is driven by processes at the intersection and the external wind direction is perpendicular to the street. The conservation equation for the concentration is:

$$d/ds(C\mathrm{H}WU_S) = q - CU_EW \ ,$$

where s is measured along the street from the intersection, q is the local line source strength, W the street width and U_E an entrainment velocity modelling mixing over the top of the canyon. The boundary condition is that $C = C_o$ at $s = 0$ and the solution, assuming U_S is constant, is:

$$C = C_o \exp(-U_E s/U_S\mathrm{H}) + \{q/U_EW\}\{1 - \exp(-U_E s/U_S\mathrm{H})\} \ ,$$

and, with $L = \mathrm{H}U_S/U_E$ defined as a decay length scale, this can be written as:

$$C = C_o \exp(-s/L) + \{q/U_EW\}\{1 - \exp(-s/L)\} \ .$$

In many of the situations studied the air flow into the lateral street was a significant fraction of that along the upwind longitudinal street; for the case shown in Figure 1 a reasonable estimate of U_S/U is 0.5. The entrainment velocity ratio, U_E/U, is likely to be of order 0.1 so that in this case the decay length scale for concentrations in the lateral street is of order L$\approx$5 H. The standard local equilibrium result for a street canyon:

$$C = q/U_EW$$

is attained once $s/L \gg 1$, emphasising again that the consequences of the air exchanges between the street at the intersection persist far into the lateral street.

Integral modelling of this sort can be considerably refined but is of limited value until linked to algorithms for the boundary conditions, C_o and Q_o (WHU$_s$). The first can probably be estimated to an acceptable accuracy from integral modelling applied to the upwind street but Q_o, being very sensitive to the geometry and wind direction, can only be defined empirically. Nevertheless, this does offer the possibility of using wind tunnel or CFD modelling to determine the behaviour of Q_o and then some form of modified street-canyon model, along the lines discussed above, to undertake a full assessment of concentrations in the vicinity of the intersection.

5. Conclusions

The results show that significant exchanges occur at intersections between two streets and that, as a consequence, pollution emitted in one street can penetrate far into the other. A further consequence is the development of persistent structure in the concentration field within a street, with receptors on opposite sides being primarily affected by entirely separate sets of sources. The exchanges are driven by minor departures from symmetry in the geometry or orientation of the intersection and are likely to be the norm in practice. As the effects of the exchanges are not confined to the immediate vicinity of the intersection, they need to be addressed in the analysis of urban air quality, whether by calculation or monitoring. The successful inclusion of such effects in dispersion models will rest heavily on the provision of a realistic empirical description of the air exchanges at the intersection and their dependence on wind direction. Such information is likely to be site-specific. Detailed studies of dispersion processes at both generic and realistic intersections are required to develop further understanding of the processes involved and to pave the way for improved dispersion models. In all probability, such research will involve both experimentation and computations (CFD).

Further analysis of the results currently available will concentrate on the effect of wind direction on the concentration field and air exchanges so that a description like that presented above can be developed for all wind directions. Annual average concentration fields can then be investigated and their sensitivity to the line source strengths in each street and the form of the wind rose established.

Acknowledgements

This work was in part funded by the UK EPSRC and the European Community through the Large Scale Facilities section of the Training and Mobility of Researcher (TMR) program, contract ERBFMGECT980117.

References

Berkowicz, R., Hertel, O., Larsen, S. E., Sørensen, N. N. and Nielsen, M.: 1997, *Modelling Traffic Pollution in Streets*, National Environmental Research Institute, Roskilde, Denmark, 52 pp., ISBN 87-7772-307-4.

Hoydysh, W. G. and Dabberdt, W. F.: 1994, 'Concentration fields at urban intersections: Fluid modelling studies', *Atmos. Environ.* **28**(11) 1849–1860.

Scaperdas, A.-S.: 2000, 'Modelling Air Flow and Pollutant Dispersion at Urban Canyon Intersections', Ph.D. Thesis, Imperial College, University of London.

Soulhac, L.: 2000, 'Modèlisation de la Dispersion Atmosphérique a l'Interieur de la Canopée Urbaine', Ph.D. Thesis, Ecole Centrale de Lyon.